LATERAL-TORSIONAL BUCKLING RESISTANCE PREDICTION OF HIGH-STRENGTH STEEL I-BEAMS WITH SINUSOIDAL WEB OPENINGS

Douglas F. SANTOS[a], Carlos H. MARTINS[b], Felipe P. V. FERREIRA[c], Konstantinos D. TSAVDARIDIS[d] and Hermano S. CARDOSO[e]

[a] Department of Civil Engineering, Federal University of São Carlos, São Carlos, Brazil
Emails: douglassantos88@hotmail.com

[b] Department of Civil Engineering, State University of Maringá, Maringá, Brazil
Emails: chmartins@uem.br

[c] Faculty of Civil Engineering, Federal University of Uberlândia, Uberlândia, Brazil
Emails: fpvferreira@ufu.br

[d] Department of Engineering, University of London, London, UK
Emails: Konstantinos.tsavdaridis@city.ac.uk

[e] ArcelorMittal Global Research and Development, Serra, Brazil
Emails: hermano.cardoso@arcelormittal.com.br

Keywords: High-strength steel; Perforated beams; Stability; Lateral-torsional buckling; Sinusoidal web opening; Residual stress; Finite element method.

Abstract. *A new cellular beam with sinusoidal shape of web openings, aka Angelina™, shows different behaviour in comparison with the standard beams with openings. It has its lateral-torsional buckling (LTB) resistance affected by residual stress in a more significant way than the beams with solid webs since the thin-walled plates are subject to the castellation process by thermal cutting and welding. The present study aims to predict the LTB resistance of high-strength steel (HSS) I-beams with sinusoidal web openings. For this, a finite element model is developed based on experimental tests, considering common and HSS. Buckling and post-buckling is performed. A parametric study is conducted by varying the strength of steel. It is expected that by increasing the strength of steel, there will be an increase in the lateral-torsional buckling resistance, mainly in the inelastic regime. The increase of the resistance for the different kind of steel analysed is proportional to the upgrade in the steel strength.*

1 INTRODUCTION

Nowadays, it is common to use steel I-beams with web openings in structural project of buildings. There are different kinds of geometric configuration for the web openings, which made possible a series of benefits when compared to the use of steel beams without web openings [1,2].

The beams with sinusoidal web openings are produced by cutting a steel I-beam or a steel plate that will be part of the web from a welded steel I-beam. The cut in a high temperature and with a sinusoidal shape is made to separate the element in two parts, which later will be welded back together. This fabrication process is similar to castellated beams, which only takes one cut in the web following a sinusoidal curve "path" [3]. Figure 1 below exemplifies the fabrication process.

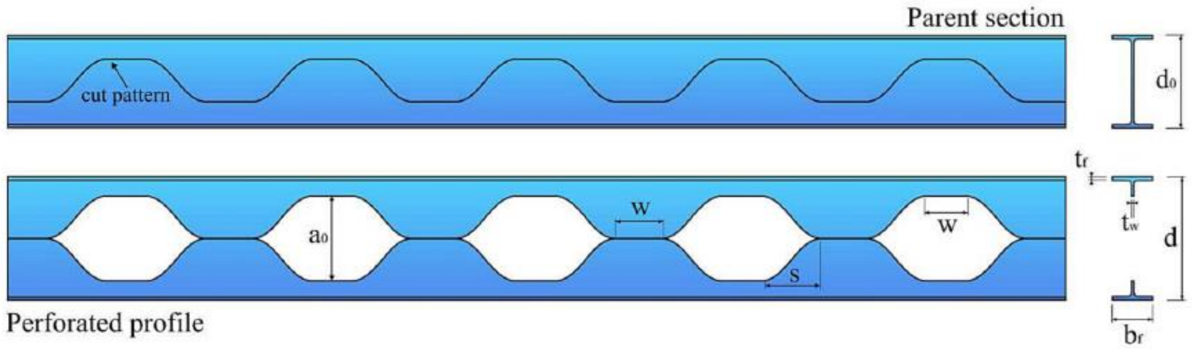

Figure 1: Fabrication scheme of beams with sinusoidal opening [1]

The possible failure modes for these beams investigated in studies such as [4,5,6]. The local failure modes are the Vierendeel mechanism which is characterized by the occurring of plastic hinges around the openings, the Web post buckling which is the local buckling of the web between the openings and Tee local buckling which is the instability of the compressed tee section on the opening part of the beam.

There are too the global failure modes, which are the Lateral-distortional buckling, Flexural mechanism and Lateral-torsional buckling, which will be the failure mode analyzed in this study [7].

In recent years, high strength steels (HSSs) have been increasingly used in construction and other industries, where the main purpose is to reduce cost and size of the members structures. Currently, 460 MPa of nominal yield stress is the number that divides the common steel to the HSS. Steels with a higher nominal yield can be considered as HSS [8,9].

In general, there are two basic types of $\sigma - \varepsilon$ curves for HSS, the curves with discontinuous yielding, i.e., with an apparent yield plateau, and the curves demonstrating continuous yielding without yield plateau [8,9], shown in figure 2. The occurrence of yield plateau depends on the fabrication process and the chemical composition of the HSS during its production. HSS tends to have to have a low ductility, and the higher the yield stress is, the ultimate strain significantly decreases. Unsafe design may happen if it is needed for the structure to work with excessive deformation. Therefore, it is important to avoid HSS reaching its fracture strain in any part of the structure [8].

To reach a high variety of cross section needed in the construction industry, welding becomes a prevailing manufacturing method for I-sections. Nevertheless, the high temperatures of the welding provoke the transformation in the microstructure of steel materials, as well as the residual stress within sections because of the local thermal expansion and contraction. Steel production techniques for HSS, such as quenching and tempering (QT) process, and thermomechanical controlled (TMCP) process, affect the mechanical behavior of steel materials near the welding seam [10,11].

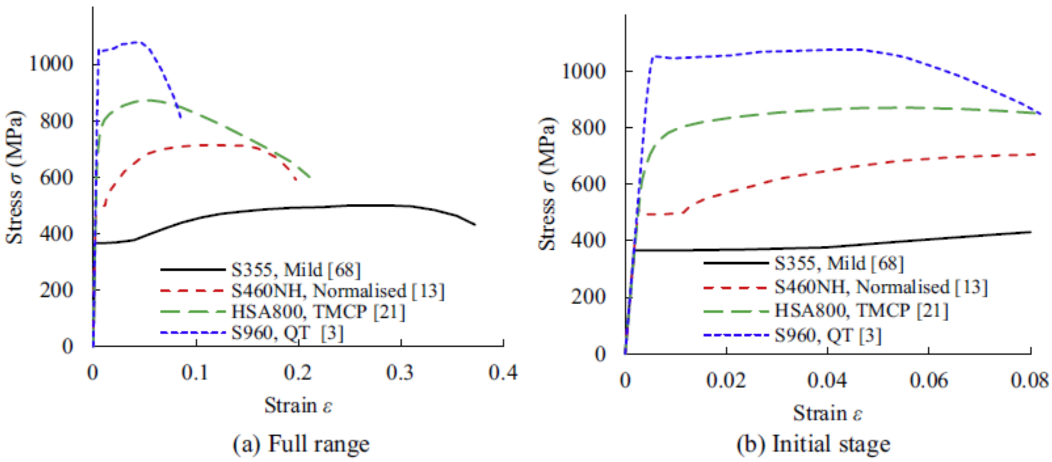

Figure 2: Comparison between stress-strain curves of different types of steel [8]

Residual stress models for hot-rolled and welded regular strength I-section steel members have been widely reported in the literature [12,13], but it is less common to find formulations for welded HSS I-sections. In a more recent studies [14,15] proposed models and formulations for welded HSS I-section. Its model was validated for steel grades S235 to S890. Most recent measurements of residual stress in welded I-section available in the literature such as [14,16-19].

Therefore, this paper aims to analyse with finite element method using ABAQUS, the LTB resistance of HSS I-section beam with sinusoidal web opening.

2 NUMERICAL MODEL

2.1 FE Model

The FE models of the I-section beams with sinusoidal web openings were developed by the commercial software ABAQUS as illustrated in figure 3. As reference, it was also simulated a beam with web opening with common strength steel ($f_y \leq 460$ MPa), in this study, it was used S355 as reference.

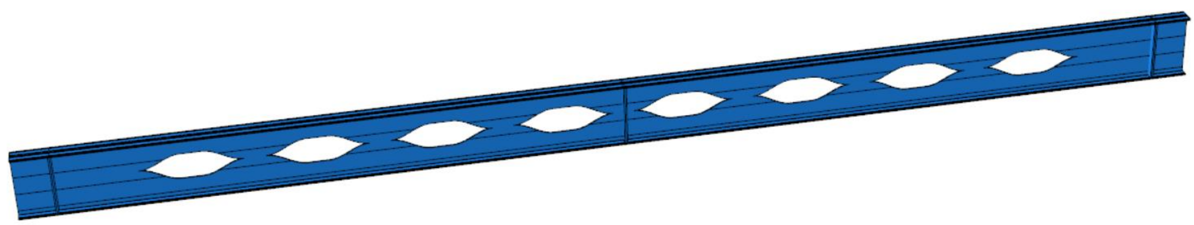

Figure 3: One of the numerical models of the HSS I-section steel beam with sinusoidal web opening

It was adopted the quadrilateral shell element with reduced integration (S4R) with mesh size of 10 mm.

A total number of 36 beams was analysed. One of the variables considered was different boundary conditions and different load conditions. It was modelled beams for 3 points and 4 points bending test. And with and without lateral restrain where the load was applied.

There were three cross-sections analysed in this study. The first two were defined to match class 1 and 2 of Eurocode 3 [20] (beams EC1 and EC2 from table 1), and the third cross section was defined following the Brazilian Standard [21] (beam NBR from table 1) to avoid local buckling of the plates from the I-section beam. The size of the cross-sections is presented at figure 4.

In addition to the variation of the boundary conditions and cross-sections, the beams were analysed following three different steel grades, S355, S500 and Q690. The combination of the variables of the 36 beams analysed is shown at table 1.

For the geometries of the openings in the web, it was used the equation (1), with the variables explained in figure 4, provided in [22].

$$y = \frac{ls}{4}\left\{sin\left[\pi\left(\frac{x}{a_0} + 1.5\right)\right] + 1\right\} \quad (1)$$

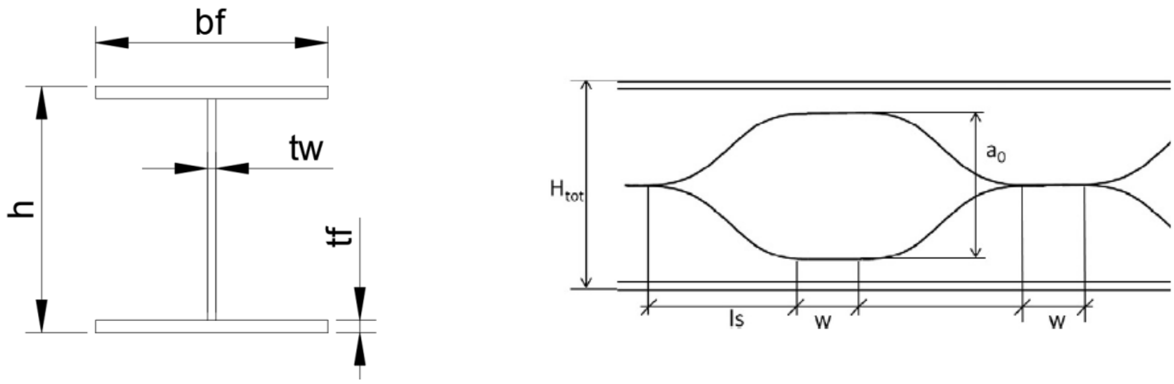

Figure 4: Cross-sections

2.2 Material characteristics

To characterize the three different steel grades, it was used the stress-strain curves provided by [8] figure 5. Table 2 summarizes the steel grades and its mechanical characteristics. For the S355 steel, it was used the values presented by [23], for S500 it was used the values provided by ArcelorMittal, which were found by experimental tests, and for the Q690 the values used was the same cited by [10]. The data of the experimental test for S500 showed it fits better in the discontinuous model. Since, it is known that S355 has the same behaviour, this model was adopted for the three steel grades.

2.3 FE Analysis

The simulations of the 36 beams were made in a two-step analysis being the first one a buckling analysis, which was used mainly to find the first positive eigenvalue. Second analysis were made using Static-Riks, so it was possible to understand through every increment, the behaviour of each beam and, using the data from the analysis to plot load-displacement curves.

It was in this second phase where it was applied in the models de geometric imperfections and residual stress, according to what was proposed by [10] and illustrated in the figure 6.

Table 1: Combination of the variables from the models analysed

Tested Beam	EC1-S355	EC1-S500	EC1-Q690	EC2-S355	EC2-S500	EC2-Q690	NBR-S355	NBR-S500	NBR-Q690
Yield Limit (MPa)	355	500	690	355	500	690	355	500	690
Parent Profile Height: h (mm)	322.5	322.5	322.5	370.5	370.5	370.5	202.5	202.5	202.5
Profile height: d (mm)	430.5	430.5	430.5	491.5	491.5	491.5	278.5	278.5	278.5
Flange Width: bf (mm)	122	122	122	136	136	136	218	218	218
Flange Thickness: tf (mm)	9.5	9.5	9.5	9.5	9.5	9.5	9.5	9.5	9.5
Web Thickness: tw (mm)	6.3	6.3	6.3	6.3	6.3	6.3	6.3	6.3	6.3
Opening height: a0 (mm)	180	180	180	205	205	205	114	114	114
Sinusoid length: ls (mm)	270	270	270	310	310	310	175	175	175
Web-post length: w (mm)	140	140	140	180	180	180	110	110	110
Beam openings number (4PBT)	9	9	9	7	7	7	13	13	13
Beam openings number (3PBT)	8	8	8	6	6	6	12	12	12
Opening length: L0 (mm)	680	680	680	800	800	800	460	460	460
Span: P (mm) Between Supports	7500	7500	7500	7500	7500	7500	7500	7500	7500
Span: PL (mm) between loads	2460	2460	2460	2940	2940	2940	2850	2850	2850
Total length of the beam: L (mm)	8000	8000	8000	8000	8000	8000	8000	8000	8000

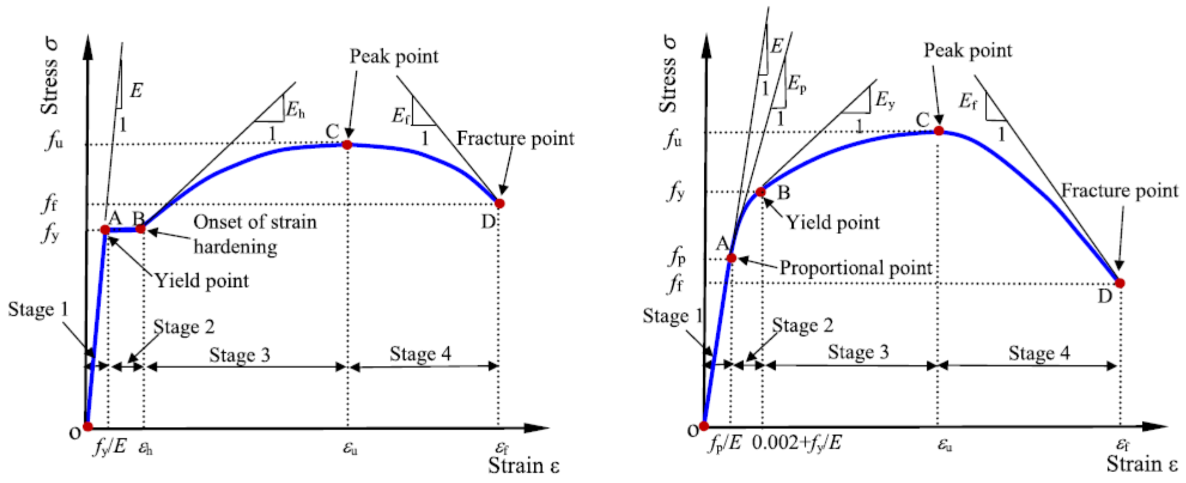

(a) Discontinuous (Model I) (b) Continuous (Model II)

Figure 5: HSS stress-strain curves proposed by [8]

Table 2: Mechanical properties for steel grades

Steel Grade	Elastic Limit f_y (MPa)	Ultimate Limit f_u (MPa)	ε_{sh} (%)	ε_u (%)	E (MPa)	Reference
S355	355	490	1.74	16.53	210000	[23]
S500	560	642.85	2.8	9.553	200000	ARCELORMITTAL
Q690	788.6	834.5	2.42	6.92	217200	[10]

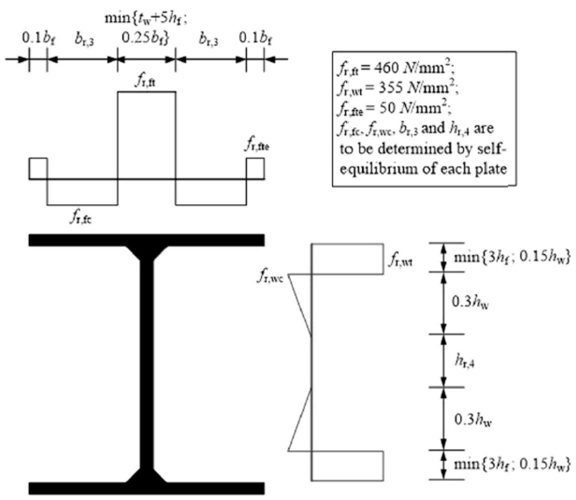

Figure 6: HSS residual stress model

3 RESULTS

After the analysis was concluded, it was possible to plot 36 curves load-displacement, as shown in figure 7 and 8, where the displacement was measured at the middle of the span in the vertical axis. The curves are classified by the boundary conditions, cross-sections and steel grades and they are illustrated in the figures 10 and 11. Figures 12 presents some deformed shapes in the analysis.

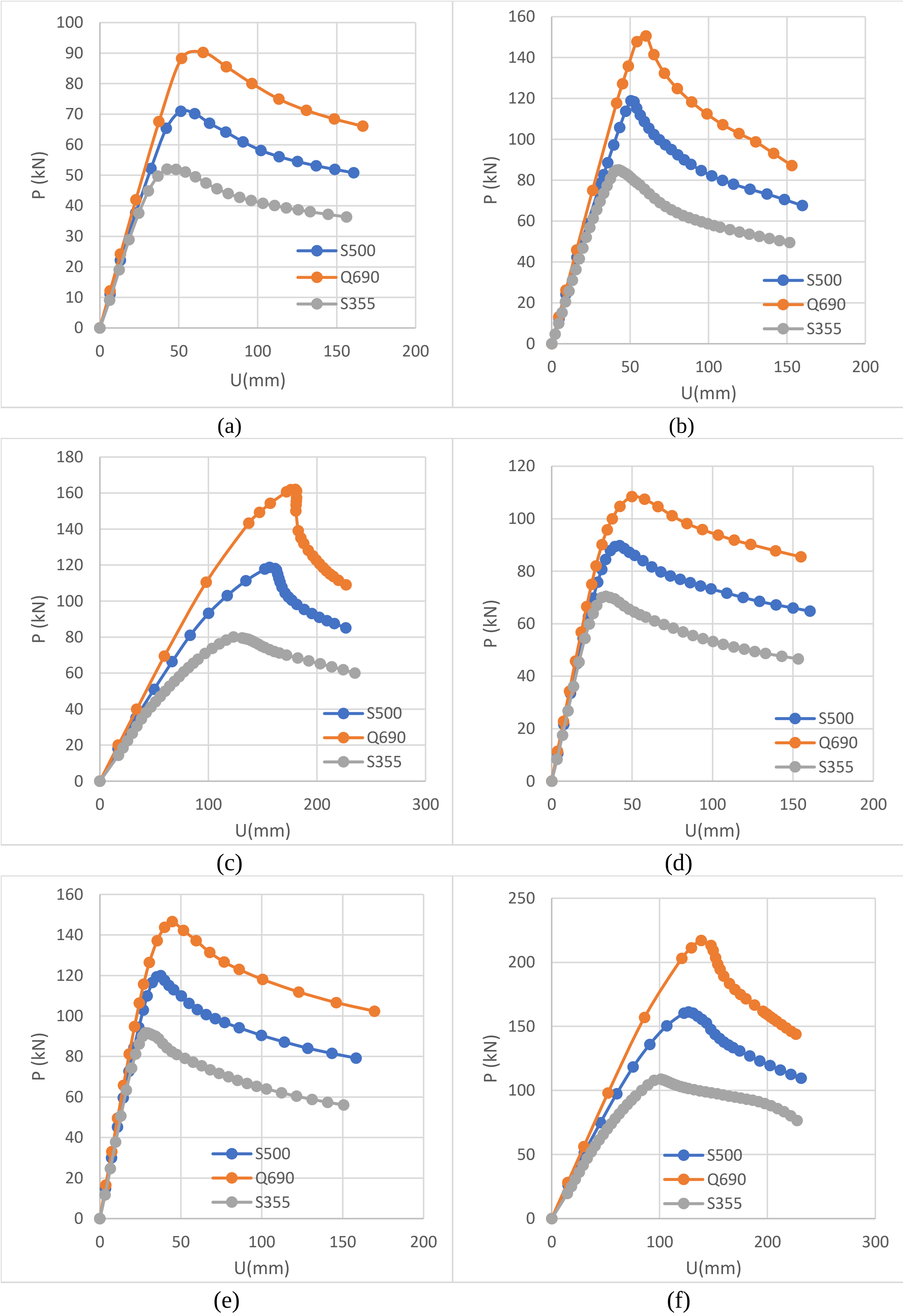

Figure 7: 4-point (a, b, c) and 3 point-bending (d, e, f) with lateral restrain tests curves for beams EC1, EC2 and NBR respectively

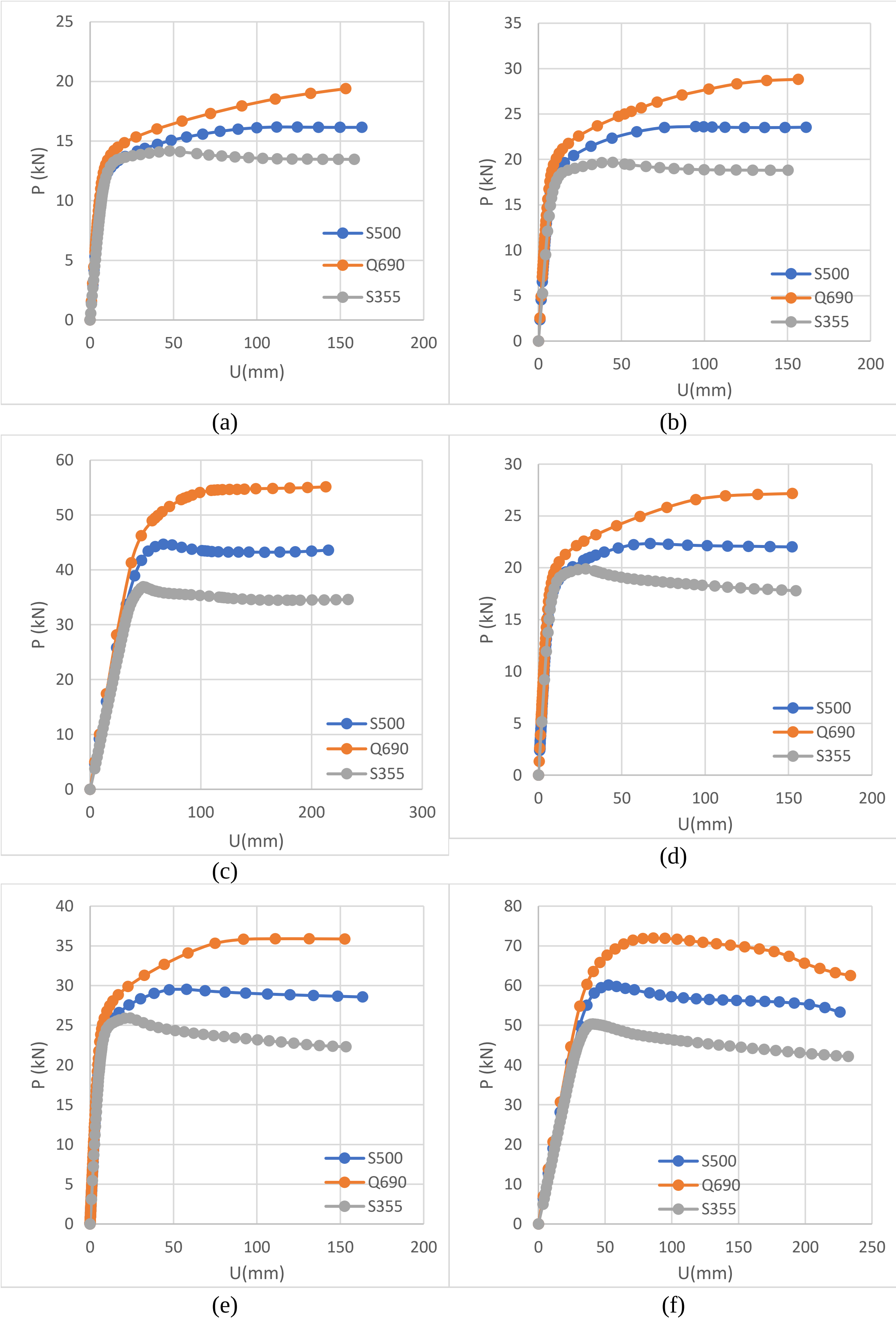

Figure 8: 4-point (a, b, c) and 3 point-bending (d, e, f) without lateral restrain tests curves for beams EC1, EC2 and NBR respectively

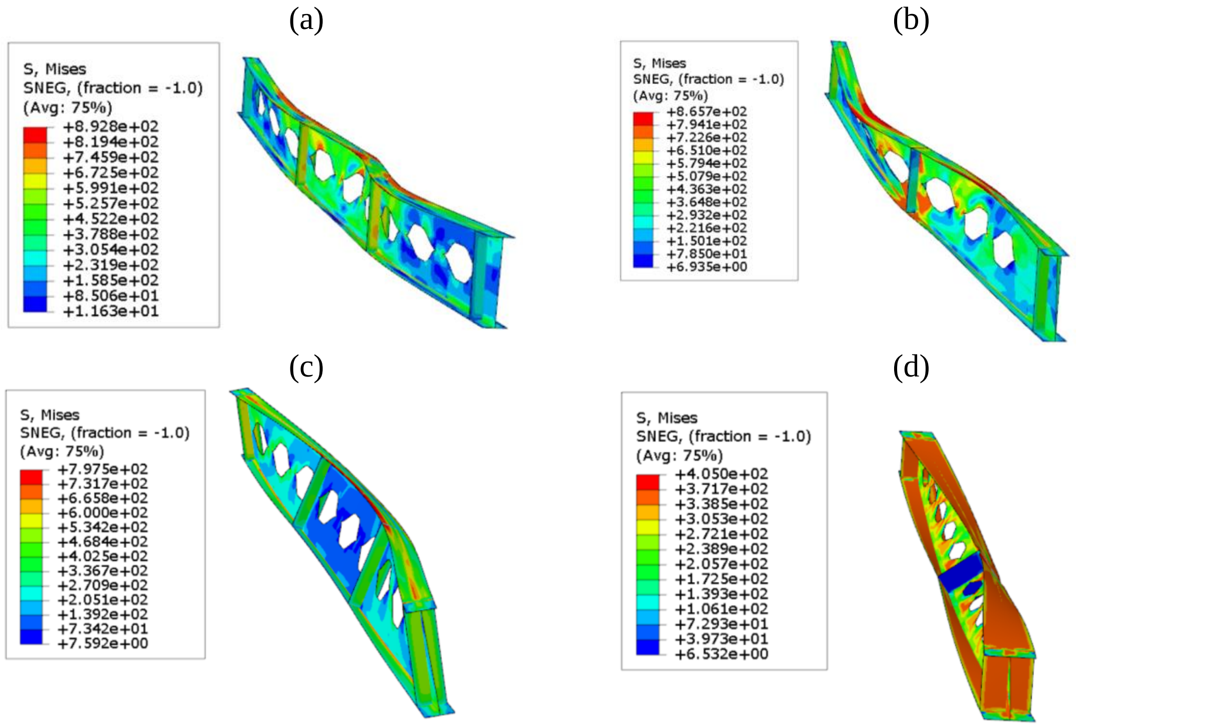

Figure 9: Some examples of deformed shapes from the analysis

4 CONCLUSION

Studying the LTB for HSS of beams with sinusoidal opening using FEM, made possible to observe through the curves of load-displacement that the yield stress impact in the resistance of the beams in the ultimate load of them. It also has an impact in the displacement measured in the middle of the span. Steel grades with higher yield stress made possible a higher displacement.

The beams with the cross-section based on the class 1 and 2 from Eurocode presented a very similar behaviour while the cross-section based on the Brazilian standard showed a different curve shape, since it was the cross-section with the smaller depth.

ACKNOWLEDGMENTS

This study was financed by the Conselho Nacional de Desenvolvimento Científico e Tecnológico (CNPq).

REFERENCES

[1] A. S. de Carvalho, C. H. Martins, A. Rossi, V. M. de Oliveira, and S. G. Morkhade, “Moment gradient factor for steel I-beams with sinusoidal web openings,” J Constr Steel Res, vol. 202, Mar. 2023, doi: 10.1016/j.jcsr.2023.107775.

[2] A. S. de Carvalho, A. Rossi, and C. H. Martins, “Assessment of lateral–torsional buckling in steel I-beams with sinusoidal web openings,” Thin-Walled Structures, vol. 175, Jun. 2022, doi: 10.1016/j.tws.2022.109242.

[3] F. Erdal and M. P. Saka, “Ultimate load carrying capacity of optimally designed steel cellular beams,” Journal of Constructional Steel Research, vol. 80. pp. 355–368, Jan. 2013. doi: 10.1016/j.jcsr.2012.10.007.

[4] S. Durif and A. Bouchaïr, “Behavior of cellular beams with sinusoidal openings,” in Procedia Engineering, Elsevier Ltd, 2012, pp. 108–113. doi: 10.1016/j.proeng.2012.07.064.

[5] S. Durif, A. Bouchaïr, and O. Vassart, "Experimental tests and numerical modeling of cellular beams with sinusoidal openings," J Constr Steel Res, vol. 82, pp. 72–87, 2013, doi: 10.1016/j.jcsr.2012.12.010.

[6] P. O. Martin, M. Couchaux, O. Vassart, and A. Bureau, "An analytical method for the resistance of cellular beams with sinusoidal openings," Eng Struct, vol. 143, pp. 113–126, Jul. 2017, doi: 10.1016/j.engstruct.2017.03.048.

[7] D. Sonck, "Global Buckling of Castellated and Cellular Steel Beams and Columns," 2013.

[8] X. Q. Wang, Z. Tao, U. Katwal, and C. Hou, "Tensile stress-strain models for high strength steels," J Constr Steel Res, vol. 186, Nov. 2021, doi: 10.1016/j.jcsr.2021.106879.

[9] G. Shi, X. Zhu, and H. Ban, "Material properties and partial factors for resistance of high-strength steels in China," J Constr Steel Res, vol. 121, pp. 65–79, Jun. 2016, doi: 10.1016/j.jcsr.2016.01.012.

[10] S. Chen, J. zhi Liu, and T. M. Chan, "Material properties and residual stresses of welded high strength steel and hybrid I-sections," Eng Struct, vol. 276, Feb. 2023, doi: 10.1016/j.engstruct.2022.115293.

[11] F. Javidan, A. Heidarpour, X. L. Zhao, C. R. Hutchinson, and J. Minkkinen, "Effect of weld on the mechanical properties of high strength and ultra-high strength steel tubes in fabricated hybrid sections," Eng Struct, vol. 118, pp. 16–27, Jul. 2016, doi: 10.1016/j.engstruct.2016.03.046.

[12] S. Shayan, K. J. R. Rasmussen, and H. Zhang, "Probabilistic modelling of residual stress in advanced analysis of steel structures," J Constr Steel Res, vol. 101, pp. 407–414, 2014, doi: 10.1016/j.jcsr.2014.05.028.

[13] L. Subramanian and D. W. White, "Resolving the disconnects between lateral torsional buckling experimental tests, test simulations and design strength equations," J Constr Steel Res, vol. 128, pp. 321–334, Jan. 2017, doi: 10.1016/j.jcsr.2016.08.009.

[14] T. Le, A. Paradowska, M. A. Bradford, X. Liu, and H. R. Valipour, "Residual stresses in welded high-strength steel I-Beams," J Constr Steel Res, vol. 167, Apr. 2020, doi: 10.1016/j.jcsr.2019.105849.

[15] L. Schaper, T. Tankova, L. Simões da Silva, and M. Knobloch, "A novel residual stress model for welded I-sections," J Constr Steel Res, vol. 188, Jan. 2022, doi: 10.1016/j.jcsr.2021.107017.

[16] B. Yang et al., "Residual stresses in welded I-shaped sections fabricated from Q460GJ structural steel plates," J Constr Steel Res, vol. 122, pp. 261–273, Jul. 2016, doi: 10.1016/j.jcsr.2016.03.029.

[17] T. J. Li, G. Q. Li, and Y. B. Wang, "Residual stress tests of welded Q690 high-strength steel box- and H-sections," J Constr Steel Res, vol. 115, pp. 283–289, Dec. 2015, doi: 10.1016/j.jcsr.2015.08.040.

[18] D. Li, A. Paradowska, B. Uy, J. Wang, and M. Khan, "Residual stresses of box and I-shaped columns fabricated from S960 ultra-high-strength steel," J Constr Steel Res, vol. 166, Mar. 2020, doi: 10.1016/j.jcsr.2019.105904.

[19] A. Su, Y. Sun, Y. Liang, and O. Zhao, "Membrane residual stresses and local buckling of S960 ultra-high strength steel welded I-section stub columns," Thin-Walled Structures, vol. 161, Apr. 2021, doi: 10.1016/j.tws.2021.107497.

[20] E. Committee for Standardisation, "EN 1993-1-1: Eurocode 3: Design of steel structures - Part 1-1: General rules and rules for buildings."

[21] Associação Brasileira de Normas Técnicas, "NBR 8800 - Projeto de Estruturas de Aço e de Estruturas Mistas de aço e Concreto de Edificios," 2008.

[22] O. Vassart, L.-G. Cajot, and J.-P. Muzeau, "Development of a new composite cellular beam," The Singapore Engineer, pp. 14–16, 2008.

[23] X. Yun and L. Gardner, "Stress-strain curves for hot-rolled steels," J Constr Steel Res, vol. 133, pp. 36–46, Jun. 2017, doi: 10.1016/j.jcsr.2017.01.024.